RSC Advances

ROYAL SOCIETY OF CHEMISTRY

www.rsc.org/advances

Simultaneous enhancement of fluorescence and solubility by *N*-alkylation and functionalization of 2-(2-thienyl)imidazo[4,5-*f*][1,10]-phenanthroline with heterocyclic bridges

Yu-Xin Peng, Na Wang, Yuan Dai, Bin Hu Bin-Bin Ma and Wei Huang*

State Key Laboratory of Coordination Chemistry, Nanjing National Laboratory of Microstructures, School of Chemistry and Chemical Engineering, Nanjing University, Nanjing 210093, P. R. China

Abstract:

A family of 2-(2-thienyl)imidazo[4,5-*f*][1,10]-phenanthroline (TIP) based compounds with large delocalized π system has been designed and synthesized by following the strategy of introducing alkyl chains and extending different *S*-, *N*- and *O*-containing aromatic heterocyclic tails. Simultaneous enhancement of fluorescence emissions and solubility in organic solvents for resultant aromatic heterocyclic compounds **1-13** has been achieved. Analyses on twelve X-ray single-crystal structures indicate that the thiophene ring of TIP unit in this series of compounds shows the same *trans* configuration with its imidazo[4,5-*f*][1,10]-phenanthroline core but different dihedral angles with adjacent aromatic heterocycles. Thermal gravimetric analyses for ten imidazole *N*-substituted TIP derivatives reveal that they still remain good thermal stability with the decomposition temperature higher than 300 °C originating from their common TIP core, even if introduction of the *n*-butyl radical in their molecular structures. Moreover, TPA and carbazole substituted compounds **2** and **9** were used as the ancillary ligands to prepare corresponding ruthenium(II) sensitizers **BM3** and **BM4**, and their dye-sensitized solar cell performance has been evaluated.

1. Introduction

In recent years, research on organic luminescent materials has attracted great attention because of their importance in the applications of light technology such as signaling, imaging and fluorescent biosensor/chemosensor materials.[1-5] Especially, materials bearing the "donor-acceptor" or "push–pull" structural architectures are more fascinating owning to their efficient absorption of

* Corresponding author. Tel.: +86–25–83686526; fax: +86–25–83314502
E–mail address: whuang@nju.edu.cn

electromagnetic radiation by virtue of an intramolecular charge transfer and emission from corresponding photoexcited state.[6-8] Consequently, considerable efforts have been conducted in designing and synthesizing diverse classes of above-mentioned fluorescent molecules.[9-14]

Among the classes of organic π system, nitrogen-containing heterocycles are very promising building blocks to synthesize a great number of strongly emissive materials.[15-18] 1,10-Phenanthroline, as a kind of common electron-deficient group, is often fused with electron-rich thiophene rings and bridged by imidazole groups. Thus, a typical donor-acceptor molecule, i.e., 2-(2-thienyl)imidazo[4,5-*f*][1,10]-phenanthroline (TIP), is formed.[19] Meanwhile, the two chelating coordinative sites of 1,10-phenanthroline are still reserved, and it makes possible the fine-tuning of optoelectronic properties in a wide range.[20-22] However, the fluorescence activity of TIP is not high enough, and it is probably caused by its short conjugated π system.

In this work, the aim of incorporating various aromatic units into the TIP backbone is to extend the conjugated π system and the rigidity of resultant molecules, thereby manipulating their electronic structures and increasing their fluorescence emissions. Considering that the aromatic heterocyclic extension is limited by the solubility of resultant molecules, which will significantly reduce their reaction activity and make them very difficult to be isolated and characterized, the alkylation strategy is used before the extension of delocalized π system. So we report herein a family of TIP based compounds following the strategy of introducing alkyl chains and extending different *S*-, *N*- and *O*-containing aromatic heterocyclic tails from α position of the TIP thiophene ring, where simultaneous enhancement of fluorescence emissions and solubility in organic solvents has been achieved. In addition, X-ray single-crystal structures of twelve compounds as well as thermal gravimetric analyses for ten imidazole *N*-substituted TIP derivatives have been explored. Moreover, TPA and carbazole substituted compounds **2** and **9** were used as the ancillary ligands to prepare corresponding ruthenium(II) sensitizers **BM3** and **BM4**, and their dye-sensitized solar cell performance has been evaluated.

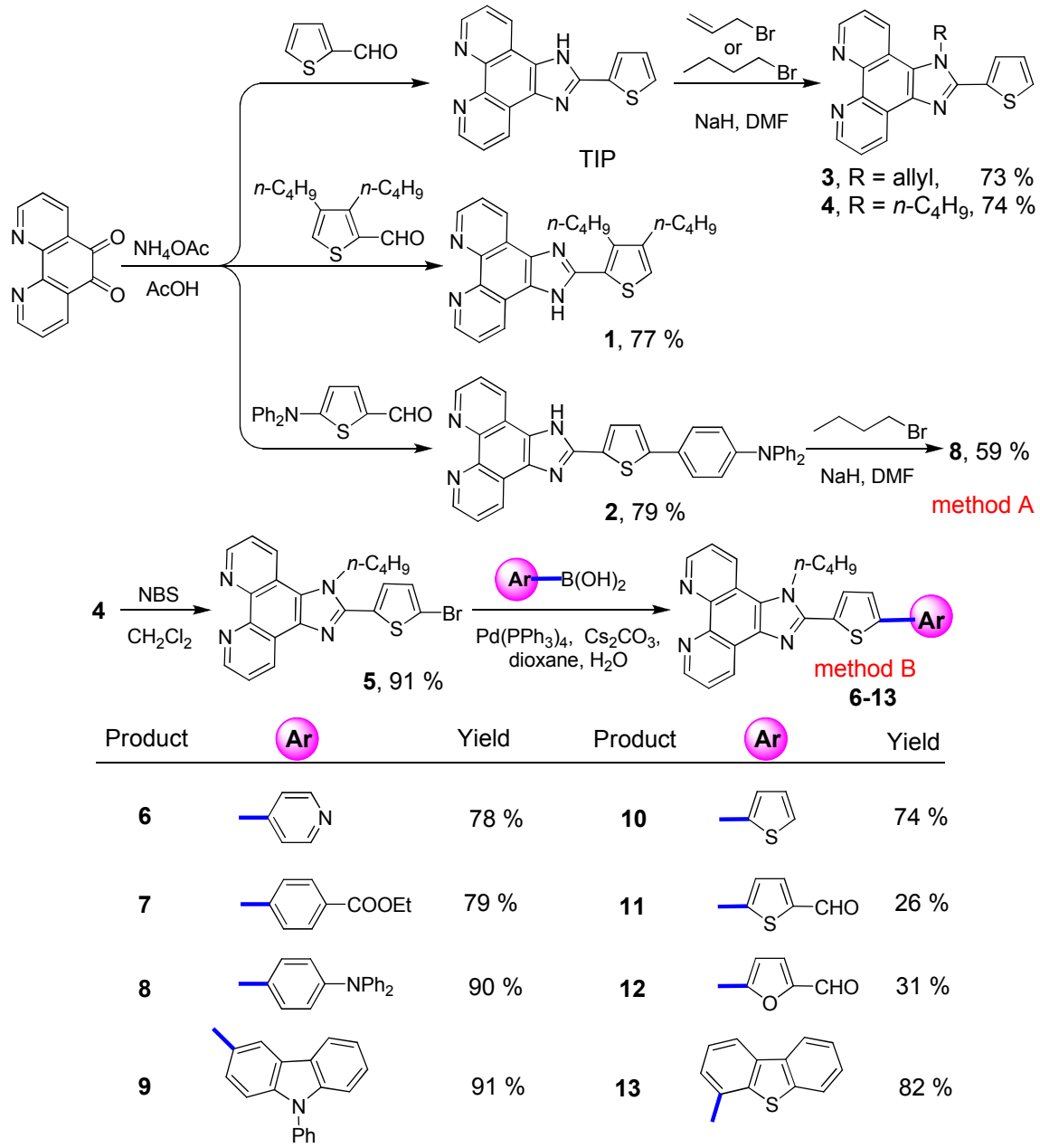

Product	Ar	Yield	Product	Ar	Yield
6		78 %	**10**		74 %
7		79 %	**11**		26 %
8		90 %	**12**		31 %
9		91 %	**13**		82 %

Scheme 1 synthetic routes for TIP based heterocyclic aromatic fluorescent compounds.

2. Results and discussion

Syntheses

Generally, Debus-Radziszewski reaction[23] between 1,10-phenanthroline-5,6-dione and corresponding formyl-thiophene derivatives in the presence of excess ammonium acetate is an effective way to construct TIP based aromatic heterocyclic compounds.[22,24-27] Herein the 2-(2-thienyl)imidazo[4,5-*f*][1,10]-phenanthroline (TIP) core was selected as the starting material for subsequent imidazole *N*-alkylation and aromatic heterocyclic extension because TIP based

derivatives including their metal complexes have shown excellent optoelectronic properties and thermal stability. As shown in Scheme 1, our synthesis started from TIP based compounds **1** and **2**, which were prepared according to Debus-Radziszewski reaction in high yields. Compared with TIP, **1** has two *n*-butyl chains in 3 and 4 positions of the thiophene ring showing better solubility in common organic solvents. However, the two crowded *n*-butyl chains have large steric hindrance effects, which will generate large dihedral angles between adjacent aromatic rings thereby influencing the extension of delocalized π system to different extents.[28-31] Actually, mono-alkylation at β position of the thiophene ring is an effective method in keeping the molecular planarity, but this strategy has the disadvantage of synthetic difficulties originating from the molecular symmetry.

As an alternative approach to increase the solubility and reaction activity of TIP based compounds including easier purification and characterization of the final products, the following *N*-alkylation reactions to obtain compounds **3** and **4** were proceeded in the presence of NaH as a base in 73 and 74 % yields, respectively. As expected, introduction of the mono-alkyl chain in compounds **3** and **4** results in an obvious improvement of solubility in common organic solvents in comparison with TIP. In our experiments, two synthetic methods (methods A and B in Scheme 1) have been used to prepare **8**, where the discrepancy between them is the sequence of *N*-alkylation and Pd-catalyzed Suzuki-Miyaura cross-coupling reactions. Our results reveal that *N*-alkylation before cross-coupling (method B) has advantages of easy-handling and even higher yields mainly owing to the increase of solubility and reaction activity. For example, in the case of compound **8**, method B gave a higher two-step yield of 56 % than method A (37 %). So method B has been used to prepare the other TIP based compounds **6-13**. Consequently, all the TIP based target compounds **6-13** bearing pyridine-, ethyl benzoate-, triphenylamino-, phenylcarbazol-, thiophene, formyl thiophene-, formyl furan- and dibenzothiophene-terminated substituents were prepared by Pd-catalyzed Suzuki-Miyaura cross-coupling reactions between intermediate **5** (obtained by the NBS bromination from **4** in CH_2Cl_2 in a 91 % yield) and corresponding boronic acids. All the reactions proceeded smoothly, which could be monitored directly by a UV-light detector excited at 365 nm with the color of fluorescence emission altering from light blue to deeper color. Furthermore, the molecular planarity of compounds **6-13** has been retained by our *N*-alkylation synthetic strategy, which could be verified by the following X-ray single-crystal structures with the dihedral angles between thiophene and its vicinal aromatic rings less than 24.4(3)°.

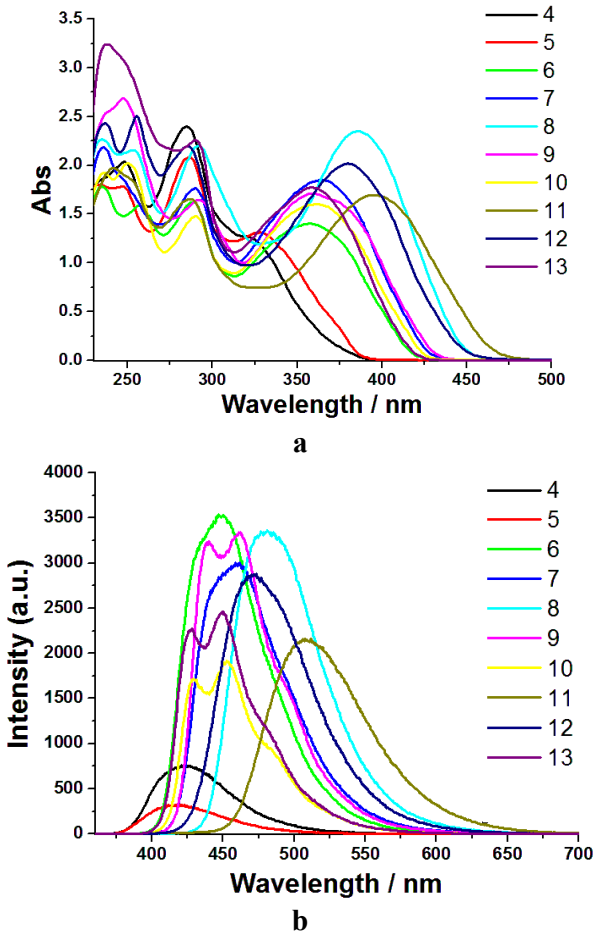

Fig. 1 UV-Vis absorption spectra (**a**) and fluorescence emission excited at 350 nm for the TIP based compounds in their CH_2Cl_2 solutions at room temperature with the same concentration of 5.0×10^{-5} mol·L^{-1}.

Spectral characterizations

The photophysical properties of TIP based compounds **4-13** in CH_2Cl_2 at a concentration of 5.0×10^{-5} M were investigated, and the spectral data were summarized in Table 2. Multiple absorption bands are observed in the UV-vis absorption spectra, as displayed in Fig. 1a. The wide peak located at 325~396 nm can be assigned as the π-π* transition absorption of conjugated system. Obviously, TIPs **6-13** with the extension of aryl radicals to α position of the thiophene ring in TIP unit exhibit not only more red-shift absorption, but also considerably enlarged the absorption area. Namely, compared with the short conjugated length in **4** (325 nm and 24800 L·mol^{-1}·cm^{-1}), compounds **6-13** have larger λ_{max} (358~396 nm) and higher ε (28100~46900 L·mol^{-1}·cm^{-1}) values. Moreover, it is also found that TIPs **6-13** show red-shift absorptions to different extents with the increase of delocalized π system for all molecules after the aromatic heterocyclic extension.

Similar to the absorption spectra, the fluorescence spectra of TIPs **6-13** also exhibit red-shift emission bands in comparison with **4**, and the photoluminescence capabilities are also strengthened

significantly. In our compounds, strong fluorescence signals are observed in compounds **6-9**, while the fluorescence emission intensity of compounds **10-13** is much weaker. It is noted that compounds **6-9** have the high Φ values of 70, 69, 73 and 72 % (Table 1), while **5** is the weakest fluorescence emitter with a Φ value of 5.0 % because of the fluorescence quenching effects of the bromo atom.[32-33] Compared with **10** having a Φ value of 38 %, its structural analogue **11** bearing an additional formyl ending group shows the higher Φ value of 46 %, and the replacement of thiophene with furan in **12** also leads to a distinct Φ value of 53 %, which agree well with previously reported uridine monophosphate derivatives with a formyl-substituted thiophene or furan ring in position 5.[34]

Table 1 UV-Vis absorption and fluorescence emission data for compounds 4-13.

Compd	UV-Vis λ_{max} [nm (eV)]	ε ($L \cdot mol^{-1} \cdot cm^{-1}$)	Fluorescence		$\Delta\lambda_{Stokes}$ (nm) [b]	Td_{10} [c] (°C)
			λ_{max} (nm)	Φ_s [a]		
4	325 (3.82)	24800	423	0.11	98	435
5	328 (3.78)	26200	416	0.05	88	374
6	358 (3.46)	28100	448	0.70	90	435
7	364 (3.41)	36900	459	0.69	95	412
8	386 (3.21)	46900	480	0.73	94	435
9	359 (3.45)	34200	462	0.72	103	470
10	362 (3.43)	32100	451	0.38	89	392
11	396 (3.13)	33900	508	0.46	112	403
12	380 (3.26)	40300	470	0.53	90	361
13	359 (3.45)	35400	449	0.37	90	463

[a] Photoluminescence quantum yields. [b] Stokes shift = λ_{max}^{em} - λ_{max}^{abs}. [c] 10 % Weight-loss temperature.

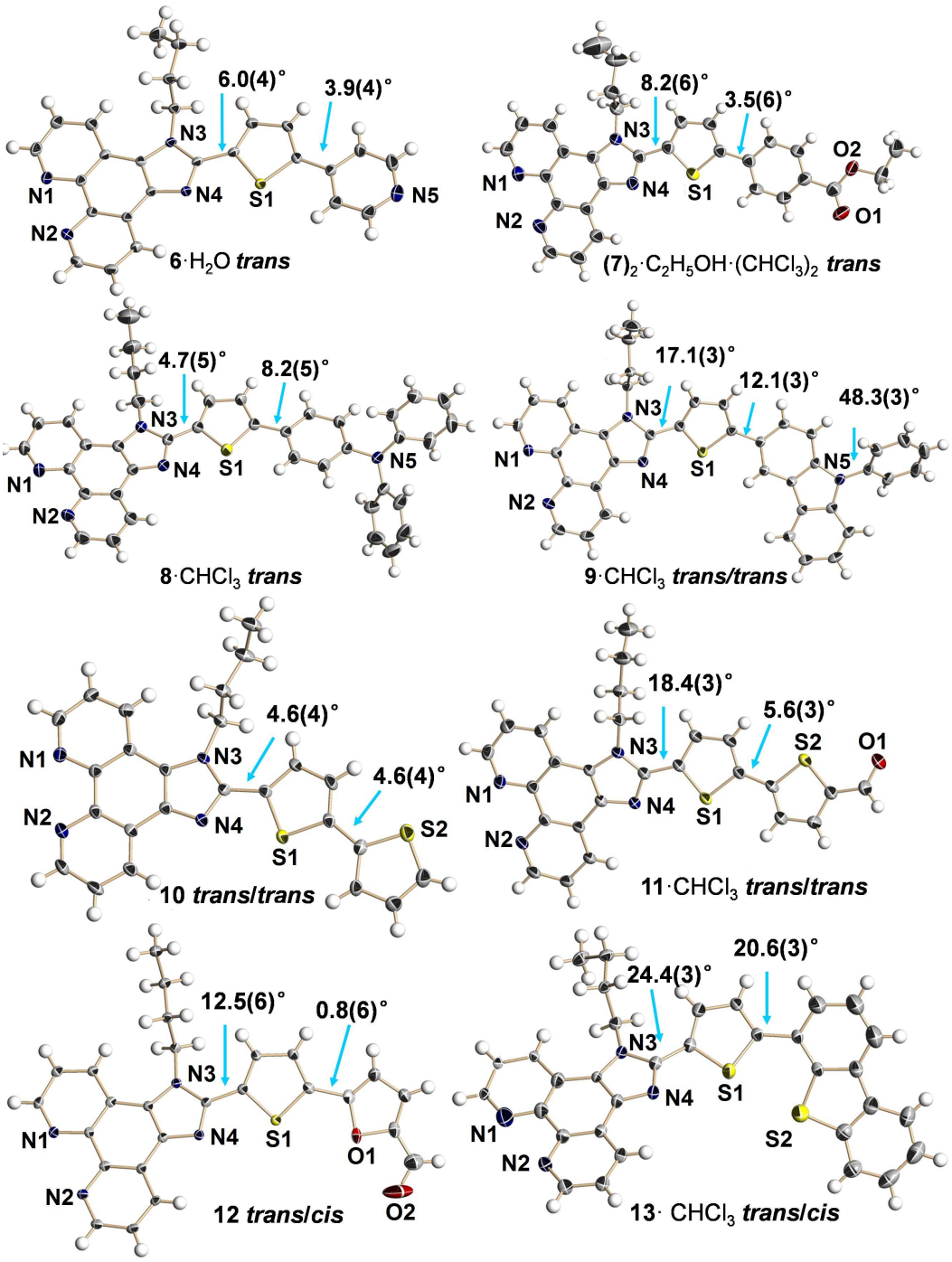

Fig. 2 ORTEP diagrams (30 % thermal probability ellipsoids) of the molecular structures of **6**·H_2O, $(\mathbf{7})_2$·C_2H_5OH·$(CHCl_3)_2$, **8**·$CHCl_3$, **9**·$CHCl_3$, **10**, **11**·$CHCl_3$, **12** and **13**·$CHCl_3$ showing the dihedral angles and relative configurations between adjacent aromatic heterocycles. All the solvent molecules are omitted for clarity.

Table 2 Crystal data and structural refinements for twelve compounds **3-13**.

Compound	**3**·$CHCl_3$	**4**	**5**·$CHCl_3$	**6**·H_2O	(**7**)$_2$·$EtOH(CHCl_3)_2$	**8**·$CHCl_3$
formula	$C_{21}H_{15}N_4SCl_3$	$C_{21}H_{18}N_4S$	$C_{22}H_{18}BrN_4S_2Cl$	$C_{26}H_{23}N_5SO$	$C_{64}H_{60}N_8O_5S_2Cl_6$	$C_{40}H_{32}N_5SCl_3$
molecular weight	461.78	358.45	556.72	453.55	1298.04	721.12
T [K]	291(2)	291(2)	291(2)	291(2)	291(2)	291(2)
wavelength / Å	0.71073	0.71073	0.71073	0.71073	0.71073	0.71073
crystal size (mm)	0.12×0.12×0.10	0.12×0.10×0.10	0.12×0.12×0.10	0.10×0.10×0.10	0.10×0.10×0.10	0.10×0.10×0.10
crystal system	triclinic	triclinic	triclinic	monoclinic	triclinic	monoclinic
space group	$P\bar{1}$	$P\bar{1}$	$P\bar{1}$	$P2_1/c$	$P\bar{1}$	$P2_1/c$
a [Å]	9.156(1)	9.713(2)	9.276(3)	16.294(2)	13.859(7)	21.993(2)
b [Å]	10.802(1)	9.923(2)	10.410(3)	7.769(1)	14.839(7)	9.058(1)
c [Å]	12.548(1)	11.205(2)	13.153(4)	19.272(2)	15.848(8)	19.520(2)
α [°]	72.798(1)	114.272(2)	107.382(5)	90	74.914(10)	90
β [°]	69.284(1)	109.020(3)	104.667(5)	116.931(6)	84.666(9)	112.815(1)
γ [°]	67.728(1)	97.147(3)	97.372(5)	90	87.572(10)	90
V [Å^3]	1055.3(10)	887.9(3)	1143.6(6)	2174.9(4)	3133(3)	3584.6(5)
Z/D_{calcd} (g/cm^3)	2 / 1.453	2 / 1.341	2 / 1.617	4 / 1.385	2 / 1.376	4 / 1.336
F(000)	472	376	560	952	1348	1496
μ [mm^{-1}]	0.549	0.194	2.257	0.179	0.397	0.351
h_{min} / h_{max}	-6 / 10	-11 / 9	-8 / 11	-15 / 19	-16 / 16	-26 / 26
k_{min} / k_{max}	-12 / 12	-11 / 11	-12 / 11	-9 / 9	-16 / 17	-10 / 9
l_{min} / l_{max}	-11 / 14	-13 / 13	-15 / 15	-22 / 22	-17 /18	-23 / 22
data / parameter	3695 / 262	3088 / 236	3915 / 309	3833 / 299	10947 / 770	6317 / 442
final R indices	R_1 = 0.0575,	R_1 = 0.0432,	R_1 = 0.0595,	R_1 = 0.0522,	R_1 = 0.0756,	R_1 = 0.0706,
[$I > 2\acute{o}(I)$]	wR_2 = 0.1502	wR_2 = 0.1313	wR_2 = 0.1526	wR_2 = 0.1161	wR_2 = 0.2019	wR_2 = 0.1754
R indices	R_1 = 0.0679,	R_1 = 0.0503,	R_1 = 0.0710,	R_1 = 0.0890,	R_1 = 0.1607,	R_1 = 0.1288,
(all data)	wR_2 = 0.1568	wR_2 = 0.1391	wR_2 = 0.1579	wR_2 = 0.1257	wR_2 = 0.2283	wR_2 = 0.1989
S	1.102	1.035	1.011	0.850	0.915	1.018
max / min $\triangle\rho$ [e·Å^{-3}]	0.775 / -0.804	0.186 / -0.380	0.846 / -0.847	0.320 / -0.395	0.649 / -0.407	0.726 / -0.614

continued

Compound	**9**·$CHCl_3$	**10**	**10**·$CHCl_3$	**11**·$CHCl_3$	**12**	**13**·$CHCl_3$
formula	$C_{40}H_{30}N_5SCl_3$	$C_{25}H_{20}N_4S_2$	$C_{26}H_{21}N_4S_2Cl_3$	$C_{27}H_{21}N_4OS_2Cl_3$	$C_{26}H_{20}N_4O_2S$	$C_{34}H_{25}N_4S_2Cl_3$
molecular weight	719.10	440.57	559.94	587.95	452.52	660.05
T [K]	291(2)	291(2)	291(2)	291(2)	291(2)	291(2)
wavelength / Å	0.71073	0.71073	0.71073	0.71073	0.71073	0.71073
crystal size (mm)	0.12×0.12×0.08	0.10×0.08×0.08	0.12×0.10×0.10	0.10×0.10×0.10	0.10×0.10×0.10	0.13×0.13×0.10
crystal system	triclinic	monoclinic	triclinic	monoclinic	monoclinic	Monoclinic
space group	$P\bar{1}$	$P2_1/c$	$P\bar{1}$	$P2_1/c$	$P2_1/c$	$P2_1/c$
a [Å]	12.404(2)	13.596(4)	9.339(1)	5.288(2)	13.767(2)	9.600(2)
b [Å]	12.454(2)	8.610(3)	12.161(2)	33.975(9)	8.367(1)	10.958(2)
c [Å]	13.762(2)	19.250(6)	12.848(2)	14.927(4)	19.124(3)	29.580(5)
α [°]	111.741(2)	90	71.990(3)	90	90	90
β [°]	100.880(3)	113.600(4)	85.936(3)	97.610(5)	108.372(2)	93.350(2)
γ [°]	110.123(2)	90	71.519(3)	90	90	90
V [Å^3]	1728.2(5)	2065.0(1)	1315.5(3)	2658.1(12)	2090.5(5)	3106.2(9)
Z/D_{calcd} (g/cm^3)	2 / 1.382	4 / 1.417	2 / 1.414	4 / 1.469	4 / 1.438	4 / 1.411
F(000)	744	920	576	1208	944	1360
μ [mm^{-1}]	0.364	0.279	0.53	0.532	0.189	0.461
h_{min} / h_{max}	-14 / 14	-16 / 16	-8 / 11	-5 / 6	-16 / 16	-11 / 11
k_{min} / k_{max}	-14 / 14	-10 / 7	-14 / 14	-40 / 40	-9 / 6	-13 / 9
l_{min} / l_{max}	-13 / 16	-22 / -22	-15 / 14	-17/ 10	-22 /22	-35 / 35
data / parameter	6017 / 471	3627 / 281	357 / 4612	4682 / 335	3654 / 299	5452 / 389
final R indices	R_1 = 0.0478,	R_1 = 0.0617,	R_1 = 0.0680,	R_1 = 0.0535,	R_1 = 0.0876,	R_1 = 0.0480,
[$I > 2\acute{o}(I)$]	wR_2 = 0.1475	wR_2 = 0.1551	wR_2 = 0.1652	wR_2 = 0.1192	wR_2 = 0.2192	wR_2 = 0.1208
R indices	R_1 = 0.0764,	R_1 = 0.1086 ,	R_1 = 0.1232,	R_1 = 0.1198,	R_1 = 0.1260 ,	R_1 = 0.0722 ,
(all data)	wR_2 = 0.1743	wR_2 = 0.1749	wR_2 = 0.1876	wR_2 = 0.1393	wR_2 = 0.2429	wR_2 = 0.1309
S	1.090	0.961	1.004	0.972	1.060	1.058
max / min $\triangle\rho$ [e·Å^{-3}]	0.272 / -0.273	0.531 / -0.465	0.415 / -0.229	0.329 / -0.282	1.358 / -0.857	0.460 / -0.410

$R_1 = \Sigma||Fo|-|Fc||/\Sigma|Fo|$, $wR_2 = [\Sigma[w(Fo^2-Fc^2)^2]/\Sigma w(Fo^2)^2]^{1/2}$

Single-crystal structures of TIP based compounds 3-13

Compared with the traditional means of characterization, X-ray single-crystal diffraction has the obvious advantages of characterizing the molecular geometry, crystal packing modes and supramolecular interactions. In this work, we have obtained single-crystal structures of eleven compounds, namely, **3**·$CHCl_3$, **4**, **6**·H_2O, (**7**)$_2$·C_2H_5OH·$(CHCl_3)_2$, **8**·$CHCl_3$, **9**·$CHCl_3$, **10**, **10**·$CHCl_3$, **11**·$CHCl_3$, **12**, **13**·$CHCl_3$ and an intermediate **5**·$CHCl_3$ (Fig. 2 and Fig. SI16). These single crystal samples suitable for X-ray diffraction were grown by slow evaporation of their solution in $CHCl_3$ or in a mixture of $CHCl_3$ and EtOH.

In comparison with the conventional double *β*-alkylation of thiophene ring, our results reveal that the single imidazole *N*-alkylation strategy for TIP based compounds has advantage of keeping the planarity of the whole molecule in addition to significantly improving the solubility, which can be clearly verified by the small dihedral angles between adjacent TIP rings in twelve X-ray single-crystal structures. In compared with the dihedral angles between imidazo[4,5-*f*][1,10]phenanthroline and their neighboring thiophene rings in synthetic precursors **3**·$CHCl_3$ and **4** (38.1(3) and 38.2(2)°), the others target TIPs **6-13**, which are terminated by various aryl groups in *α* position of the thiophene ring in the TIP core, show smaller dihedral angles in the range of 4.6(4)~24.4(3)°, indicating that the introduction of one *n*-butyl group in the imidazole ring does not destroy too much the planarity of TIP based molecules. The observation on the dihedral angle discrepancy for compounds **6-13** before and after aromatic heterocyclic extension is consistent with their afore-mentioned fluorescence emission varaitions. In addition, the alkyl substituted nitrogen atom in the TIP unit and its neighboring sulfur atom of the thiophene ring are found to point to the opposite directions, exhibiting the common *trans* configuration. The crystal packing view of this family of TIPs is shown in Fig. SI17, where typical intermolecular *π*-*π* stacking interactions are found between adjacent aromatic rings.

Thermal stability

Thermal properties of all the powder samples of *n*-butyl containing TIP based compounds **4-13** have been further investigated by thermal gravimetric analysis (TGA) for comparisons. As depicted in Fig. 3, all compounds, except **8** which may be impacted by the solvate $CHCl_3$, display excellent thermal stability with the

decomposition temperature high than 300 °C, and the Td_{10} values range from 374 to 463 °C. It is worthwhile mentioning that phenylcarbazol- and dibenzothiophene-terminated TIPs **9** and **13** exhibit the best thermal stability. It is concluded that all the TIP derivatives bearing different terminating chromophores in α position of the thiophene ring still remain good thermal stabilities even if introduction of the *n*-butyl radical in the imidazole ring for better solubility and easier purification.

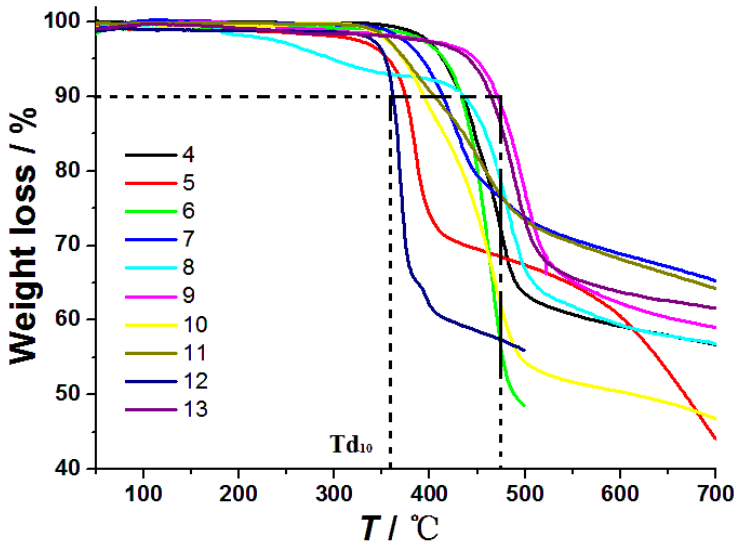

Fig. 3 Thermograms of all *n*-butyl containing TIP based compounds **4-13**.

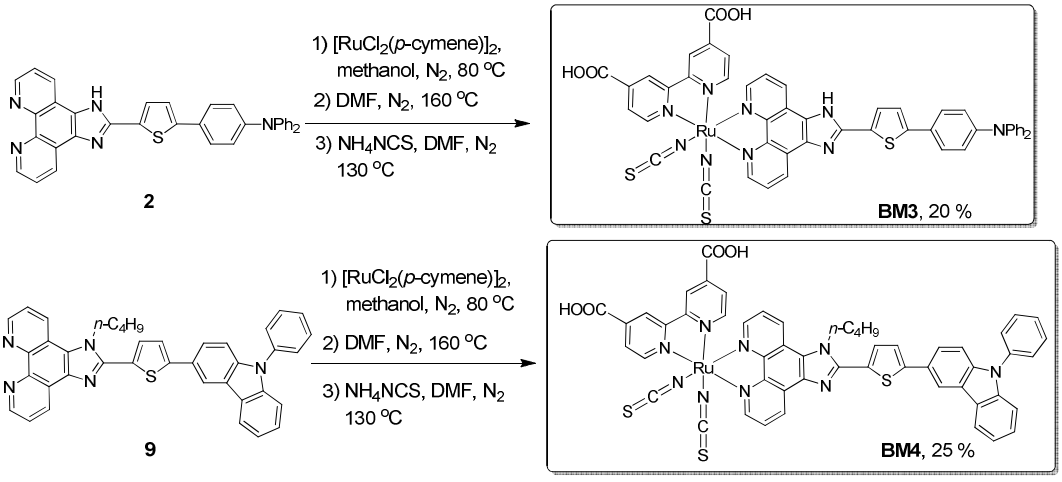

Scheme 2 Synthetic route for two ruthenium sensitizers **BM3** and **BM4**.

Dye-sensitized solar cell performance of ruthenium(II) sensitizers containing TPA and carbazole substituted ancillary ligands

In recent years, ruthenium complexes containing 1,10-phenanthroline based ancillary ligands have been used for the studies of dye-sensitized solar cells (DSCs).[35-38] In particular, TPA and carbazole involved ancillary ligands have shown good DSC performances[39-41] with high power-conversion efficiencies (PCEs). So in this work, TPA and carbazole substituted compounds **2** and **9** were used as the ancillary ligands to react with half molar ratio of $[RuCl_2(p\text{-cymene})]_2$ and then excess ammonium thiocyanate to produce corresponding ruthenium(II) sensitizers **BM3** and **BM4**. In comparison with ligands **2** and **9**, **BM3** and **BM4** display a new UV-vis absorption peak at 527 and 521 nm (Fig. 4a), respectively, indicative of typical metal-to-ligand charge transfer within molecules.

The photocurrent density-voltage curves and incident photon-to-current efficiency (IPCE) spectra of **BM3** and **BM4** under the AM1.5 sunlight illumination are shown in Fig. 4b and Fig. 4c, respectively, together with our recently reported ruthenium(II) sensitizer **BM1**[42] containing a carbazole teminated TIP ancillary ligand in the absence of an alkyl chain for comparison. It is noted that **BM4** based DSC has a relatively low PCE value of 4.62 % than that of **BM1** after the introduction of *n*-butyl group at the imidazole nitrogen atom under the same cell fabrication and efficiency measuring procedures, which is consistent with the results of their IPCE spectra. In addition, the DSC fabricated from TPA based ruthenium(II) sensitizer **BM3** shows a much lower PCE value of 4.01 % and open-circuit voltage of 0.61 V. Our results indicate that the phenylcarbazol tail is better than the triphenylamino one in their PCEs of corresponding DSCs and the introduction of a long alkyl chain into the imidazole unit of TIP based molecule cannot improve efficiently the overall DSC performance.

Table 3 Optical data and cell performance of two ligands and three sensitizers.

Sensitizer	λ_{max}/nm [a] π–π^*, π–π^* or 4d–π^*, 4d–π^*	J_{sc} (mA·cm^{-2})	V_{oc} (V)	FF [b]	η (%) [c]
2	293, 410				
9	299, 359				
BM1	301, 385, 525	16.50	0.69	64.1	7.34
BM3	299, 401, 527	9.45	0.61	69.2	4.01
BM4	299, 363, 521	9.93	0.69	67.4	4.62

[a] Absorption maxima. [b] FF = fill factor. [c] The power conversion efficiency of

N3-sensitized solar cell (where N3 is $[Ru(dcbpy)_2(NCS)_2]$) measured by the same device fabrication process is 6.07%.

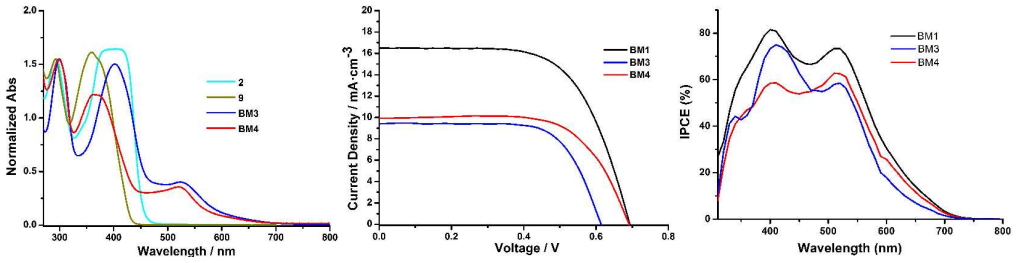

a **b** **c**

Fig. 4 (**a**) UV-Vis absorption spectra for **2**, **9**, **BM3** and **BM4** in their DMF solutions. (**b**) and (**c**) Current density-voltage characteristics and IPCE spectra of the photovoltaic devices with different photosensitizers under the AM1.5 simulated sunlight (100 $mW \cdot cm^{-2}$) illumination (thickness of TiO_2 = 12 μm; cell active area = 0.16 cm^2).

3. Conclusion

In summary, we have described herein a group of TIP based heterocyclic aromatic fluorescent compounds including imidazole *N*-substituted alkyl chains (allyl and *n*-butyl). Synthetic, spectral, structural and thermal studies have been made to reveal the influences of *N*-alkylation and aromatic heterocyclic extension on the resultant TIP derivatives. It is concluded that simultaneous enhancement of fluorescence and solubility by *N*-alkylation and the following aromatic heterocyclic extension has been achieved for this series of heterocyclic aromatic compounds. In addition, good molecular planarity and thermal stability for the resultant aromatic heterocyclic extended TIPs can be retained by means of our synthetic strategy even if introduction of the alkyl radical for better solubility and easier purification, which can be verified by the small dihedral angles between adjacent aromatic rings in nine X-ray single-crystal structures (< 24.4(3)°) and the high decomposition temperature (> 300 °C), respectively. Furthermore, TPA and carbazole substituted compounds **2** and **9** have been used as the ancillary ligands to prepare corresponding ruthenium(II) sensitizers **BM3** and **BM4**, and their DSC performance have been evaluated.

4. Experimental section

Materials and measurements

The synthetic details and characterization of 1,10-phenanthroline-5,6-dione,[43] 3,4-dibutylthiophene-2-carbaldehyde[44] and 2-triphenylamine-thiophene-5-carbaldehyde[45] have been previously reported. Unless otherwise specified, solvent of analytical grade was purchased from commercial sources and used as received. Column chromatography was carried out on silica gel (300~400 mesh). Standard techniques for synthesis were carried out under argon atmosphere. All melting points were measured without any corrections.

^{1}H and ^{13}C NMR spectroscopic measurements were performed on a Bruker AM-500 NMR spectrometer using TMS ($SiMe_4$) as an internal reference at room temperature. Electroionization mass spectra (EI-MS, electron energy 70 eV) were recorded by GCT TOF mass spectrometer (Micromass, Manchester, UK). Electrospray ionization mass spectra (ESI-MS) were recorded by a ThermoFisher Scientific LCQ Fleet mass spectrometer in a scan range of 200~2000 amu. Electrospray ionization mass spectra (ESI-MS) were recorded by a ThermoFisher Scientific LCQ Fleet mass spectrometer in a scan range of 100-2000 amu. Infrared (IR) spectra (4000~400 cm^{-1}) were recorded using a Nicolet FT-IR 170X spectrophotometer on KBr disks. UV-Vis spectra were recorded with a Shimadzu UV-3150 double-beam spectrophotometer using a quartz glass cell with a path length of 10 mm. Elemental analyses (EA) for carbon, hydrogen and nitrogen were performed on a Perkin-Elmer 1400C analyzer. Luminescence spectra were recorded on an F-4600 fluorescence spectrophotometer at room temperature. Thermogravimetry analyses were carried out by a NETZSCH STA449C thermogravimetric analyzer in the nitrogen flow from 50 to 700□ at a heating rate of 10.0 °C/min.

$$\Phi_s = \Phi_{std}\left(\frac{I_s}{I_{std}}\right)\left(\frac{A_{std}}{A_s}\right)\left(\frac{\eta_s}{\eta_{std}}\right) \qquad \text{Eq. (1)}$$

Luminescence spectra were recorded on fluorescence spectrophotometer at room temperature (25°C) using the same solutions as those for the UV-Vis determination. Fluorescence quantum yield gives the efficiency of the fluorescence process, and the

popular method to calculate it is to compare the fluorescence intensities (integrated areas) of a standard sample and the unknown one using the following equation. As can be seen in Eq. (1), Φ_s is the luminescence quantum yield of the unknown sample, Φ_{std} is the luminescence quantum yield of the standard substance, I is the wavelength-integrated area of the corrected emission spectrum, and A is the absorbance value at the excitation wavelength. The η_s and η_{std} terms represent the refractive indices of the corresponding solvents (pure solvents were assumed). We use anthracene in its ethanol solution as a standard sample (Φ_{std} = 27.0 %, η_{std} = 1.36),[46] and TIP based compounds **4-13** were dissolved in CH_2Cl_2 (η_s = 1.42).

Photovoltaic measurements were recorded with a Newport Oriel solar simulator (Model 91160) equipped with a class a xenon light source powered by a Newport power supply. The power output of the lamp was measured to 1 Sun (100 $mW \cdot cm^{-2}$) using a certified Si reference cell. The current-voltage ($I-V$) characteristic of each cell was obtained by applying an external potential bias to the cell and measuring the generated photocurrent with a Keithley digital source meter (Model 2400).

X-ray data collection and structural determination

Single-crystal samples of twelve compounds were covered with glue and mounted on glass fibers and then used for data collection. The crystal system was determined by Laue symmetry and the space groups were assigned on the basis of systematic absences using XPREP. Absorption correction was performed to the data and the structures were solved by direct methods and refined by full-matrix least-squares method on F_{obs}^2 by using the SHELXTL-PC software package.[47-48]All non-H atoms were anisotropically refined and all hydrogen atoms were inserted in the calculated positions assigned fixed isotropic thermal parameters and allowed to ride on their respective parent atoms. The summary of the crystal data, experimental details and refinement results for all twelve compounds is listed in Table 2, whereas selected bond distances and angles are given in Table SI1.

Syntheses and characterizations of compounds 1-13:

Compound **1**: 1,10-Phenanthroline-5,6-dione (1.00 g, 4.76 mmol), 3,4-dibutylthiophene-2-carbaldehyde (1.07 g, 4.77 mmol) and ammonium acetate (3.67 g, 47.61 mmol) were dissolved in 150 mL acetic acid. The mixture was heated to 100 ℃ for 10 h, cooled to room temperature, neutralized with 25 % NH_3 solution

and extracted by 200 mL $CHCl_3$. The organic layer was collected, dried over anhydrous Na_2SO_4 and concentrated in a vacuum. Compound **1** was finally separated by silica gel column chromatography using $CHCl_3$ as the eluent to give light yellow solid in a yield of 1.52 g (77 %). Mp: 184-186 °C. Main FT-IR absorptions (KBr pellets, cm^{-1}): 3420 (vs), 2957 (m), 2922 (m), 2854 (w), 1643 (m), 1564 (m), 1497 (m), 1433 (m), 1401 (m), 1347 (m), 1190 (w), 1071 (w), 1034 (w), 808 (m), 739 (s). ^1H NMR (500 MHz, $CDCl_3$) δ: 8.96 (m, 4H, phen), 7.58 (m, 2H, phen), 6.86 (s, 1H thiophene), 3.07 (m, 2H, *n*-butyl), 2.49 (m, 2H, *n*-butyl), 1.59 (m, 4H, *n*-butyl), 1.41 (m, 4H, *n*-butyl), 0.93 (m, 6H, *n*-butyl). ^{13}C NMR (125 MHz, $CDCl_3$) δ: 147.5, 147.3, 144.0, 143.6, 142.8, 131.0, 126.0, 123.2, 121.3, 32.4, 31.8, 28.6, 7.5, 23.0, 22.5, 13.9. EI-TOF-MS (*m/z*): Calcd for $[C_{25}H_{26}N_4S]^+$ 414.2 (100.0 %), found 414.2 (68.5 %). *Anal.* calcd for $C_{25}H_{26}N_4S$: C, 72.43; H, 6.32; N, 13.51 %. Found: C, 72.17; H, 6.11; N, 13.24 %.

Compound **2**: 1,10-Phenanthroline-5,6-dione (1.00 g, 4.76 mmol), 2-triphenylamine-thiophene-5-carbaldehyde (1.60 g, 4.77 mmol) and ammonium acetate (3.67 g, 47.61 mmol) were dissolved in 200 mL acetic acid. The mixture was heated to 100 °C for 4 h, cooled to room temperature, transferred to an ice bath and neutralized with ammonia until no more precipitate turned up. The precipitate was filtered under reduced pressure, washed by excess water and anhydrous ether, and dried in vacuo to give **2** as yellow solid in a yield of 2.05 g (79 %) . Mp: > 300 °C. Main FT-IR absorptions (KBr pellets, cm^{-1}): 3467 (vs), 1688 (m), 1522 (m), 1189 (w), 631 (m). ^1H NMR (500 MHz, DMSO-d_6) δ: 13.86 (s, 1H, imidazole), 9.04 (s, 2H, phen), 8.86 (m, 2H, phen), 7.88-7.80 (m, 2H; phen + 1H, thiophene), 7.70 (d, 2H, J = 8.2 Hz, triphenylamine), 7.57 (d, 1H, J = 3.4 Hz, thiophene), 7.36 (m, 4H, triphenylamine), 7.11 (m, 6H, triphenylamine), 7.03 (d, 2H, J = 8.2 Hz, triphenylamine). ^{13}C NMR (125 MHz, DMSO-d_6) δ: 148.2, 147.7, 147.1, 146.6, 145.3, 143.9, 131.9, 130.1, 129.9, 127.7, 127.3, 127.0, 124.9, 124.0, 123.7, 123.1. EI-TOF-MS (*m/z*): Calcd for $[C_{35}H_{23}N_5S]^+$ 545.2 (100.0 %), found 545.1 (100.0 %). *Anal.* calcd for $C_{35}H_{23}N_5S$: C, 77.04; H, 4.25; N, 12.83 %. Found: C, 76.91; H, 4.43; N, 12.58 %.

Compound **3**: To a DMF (100 mL) solution of TIP (1.00 g, 3.31 mmol) was added NaH (0.24 g, 10.00 mmol) and allyl bromide (2.00 g, 16.55 mmol). The resulting solution was stirred for 0.5 h at room temperature and heated to 105 °C for 12 h under argon atmosphere. The reaction mixture was then cooled to room temperature and

quenched with distilled water. The solvent was removed under reduced pressure, and then the residue was dissolved in 200 mL $CHCl_3$ and rinsed by distilled water three times. The organic layer was collected, dried over anhydrous Na_2SO_4 and concentrated in a vacuum. The desired compound **3** was finally separated by silica gel column chromatography using $CHCl_3$ as the eluent to give light yellow solid in a yield of 0.83 g (73 %). Light yellow single crystals of **3** suitable for X-ray diffraction measurement were obtained from $CHCl_3$ by slow evaporation in air at room temperature for 4 days. Mp: 196-198 °C. Main FT-IR absorptions (KBr pellets, cm^{-1}): 3016 (m), 2956 (m), 2868 (m), 1598 (w), 1564 (m), 1469 (s), 1394 (m), 1355 (m), 1155 (m), 1083 (m), 798 (m), 740 (s), 711 (m). ^{1}H NMR (500 MHz, $CDCl_3$) δ: 9.19 (dd, 1H, J = 3.4, 1.2 Hz, phen), 9.16 (d, 1H, J = 3.4 Hz, phen), 9.10 (dd, 1H, J = 6.5, 1.1 Hz, phen), 8.55 (d, 1H, J = 6.7 Hz, phen), 7.73(m, 1H, phen), 7.64 (m, 1H, phen), 7.58 (d, 1H, J = 4.0 Hz, thiophene), 7.55 (d, 1H, J = 2.8 Hz, thiophene), 7.21 (m, 1H, thiophene), 6.38 (m, 1H, thiophene), 5.53 (d, 1H, J = 8.6 Hz, allyl), 5.34 (d, 2H, J = 1.8 Hz, allyl), 5.20 (d, 1H, J = 13.8 Hz, allyl). ^{13}C NMR (125 MHz, $CDCl_3$) δ: 148.9, 147.7, 144.6, 144.1, 136.4, 132.0, 131.3, 130.5, 128.8, 128.3, 127.9, 127.8, 125.8, 123.8, 123.4, 122.4, 119.3, 118.3, 49.3. ESI-MS (*m/z*): Calcd for $[C_{20}H_{14}N_4S]^+$ 342.1 (100.0 %), found: $[M + 1]^+$ 343.3 (100.0 %). *Anal.* calcd for $C_{20}H_{14}N_4S$: C, 70.15; H, 4.12; N, 16.36 %. Found: C, 70.01; H, 4.23; N, 16.17 %.

Compound **4**: The synthetic procedure for **3** was followed using TIP (4.00 g, 13.24 mmol), NaH (0.96 g, 40.00 mmol), 1-bromobutane (9.08 g, 66.26 mmol) and DMF (250 mL). Compound **4** was obtained as light yellow solid in a yield of 3.52 g (74 %). Light yellow single crystals of **4** suitable for X-ray diffraction measurement were obtained from $CHCl_3$ by slow evaporation in air at room temperature for 1 day. Mp: 174-176 °C. Main FT-IR absorptions (KBr pellets, cm^{-1}): 3022 (m), 2960 (w), 2869 (w), 1595 (w), 1562 (m), 1514 (w), 1465 (s), 1396 (m), 1355 (m), 1155 (m), 1083 (m), 974 (w), 941 (w), 848 (w), 796 (s), 738 (s), 711 (s), 615 (w). ^{1}H NMR (500 MHz, $CDCl_3$) δ: 9.18 (m, 2H, phen), 9.08 (dd, 1H, J = 10.2, 2.2 Hz, phen), 8.57 (dd, 1H, J = 10.5, 1.8 Hz, phen), 7.71 (m, 2H, phen), 7.60 (dd, 1H, J = 5.1, 1.0 Hz, thiophene), 7.56 (dd, 1H, J = 3.6, 1.0 Hz, thiophene), 7.25 (dd, 1H, J = 5.1, 3.6 Hz, thiophene), 4.72 (m, 2H, *n*-butyl), 2.05 (m, 2H, *n*-butyl), 1.49 (m, 2H, *n*-butyl), 1.00 (m, 3H, *n*-butyl). ^{13}C NMR (125 MHz, $CDCl_3$) δ: 148.9, 147.6, 147.2, 144.7, 144.1, 136.6, 131.5, 130.5, 128.6, 128.6, 127.8, 125.1, 123.9, 123.4, 122.6, 119.8, 46.7, 32.2, 19.7, 13.6. EI-TOF-MS (*m/z*): Calcd for $[C_{21}H_{18}N_4S]^+$ 358.1 (100.0 %), found 358.2

(100.0 %). *Anal.* calcd for $C_{21}H_{18}N_4S$: *Anal.* calcd for $C_{46}H_{32}N_4S_3$: C, 70.36; H, 5.06; N, 15.63 %. Found: C, 70.19; H, 5.11; N, 15.43 %.

Compound **8**: The synthetic procedure for **3** was followed using **2** (0.50 g, 0.92 mmol), NaH (0.07 g, 2.92 mmol), 1-bromobutane (0.63 g, 4.60 mmol) and DMF (100 mL). *Compound* **8** was obtained as yellowish-green solid in a yield of 0.33 g (59 %). Yellow single crystals of compound **8** suitable for X-ray diffraction determination were grown from a solution of $CHCl_3$ by slow evaporation in air at room temperature for 3 days. Mp: 223-225 °C. Main FT-IR absorptions (KBr pellets, cm^{-1}): 3030 (w), 2964 (w), 2931 (w), 2873 (w), 1589 (s), 1485 (s), 1396 (w), 1323 (m), 1282 (s), 1172 (w), 1080 (w), 804 (m), 746 (m), 698 (m), 621 (w). ^{1}H NMR (500 MHz, $CDCl_3$) δ: 9.16 (m, 2H, phen), 9.08 (d, 1H, phen), 8.57 (m, 2H, phen), 7.71 (m, 2H, phen), 7.56 (d, 2H, J = 8.5 Hz, triphenylamine), 7.49 (d, 1H, J = 3.8 Hz, thiophene), 7.33 (d, 1H, J = 3.8 Hz, thiophene), 7.30 (m, 4H, triphenylamine), 7.16 (m, 4H, triphenylamine), 7.12 (d, 2H, J = 8.6 Hz, triphenylamine), 7.07 (m, 2H, triphenylamine), 4.77 (m, 2H, *n*-butyl), 2.07 (m, 2H, *n*-butyl), 1.54 (m, 2H, *n*-butyl), 1.02 (m, 3H, *n*-butyl). ^{13}C NMR (125 MHz, $CDCl_3$) δ: 149.0, 148.1, 147.6, 147.5, 147.4, 147.3, 144.7, 144.1, 136.8, 135.4, 130.6, 129.4, 129.2, 127.9, 127.9, 126.8, 125.3, 124.8, 124.7, 123.9, 123.5, 123.5, 123.2, 123.0, 122.7, 122.6, 122.3, 119.9, 46.9, 32.3, 19.8, 13.7. EI-TOF-MS (*m/z*): Calcd for $[C_{39}H_{31}N_5S]^+$ 601.2 (100.0 %), found 601.4 (100.0 %). *Anal.* calcd for $C_{39}H_{31}N_5S$: C, 77.84; H, 5.19; N, 11.64 %. Found: C, 77.65; H, 5.14; N, 11.44 %.

Compound **5**: In the absence of light, NBS (1.52 g, 8.54 mmol) was dissolved in CH_2Cl_2 (10 mL) and injected into a solution of compound **4** (3.00 g, 8.38 mmol) in CH_2Cl_2 (20 mL) under argon atmosphere. The mixture was refluxed for 5 h, and the resulting slurry was cooled to 0 °C and filtered. The solid was rinsed with distilled water, recrystallized from $CHCl_3$-hexane, and dried in a vacuum to give pure compound **5** as light yellow solid (3.34 g, 91 %). Light yellow single crystals of **5** suitable for X-ray diffraction measurement were obtained from $CHCl_3$ by slow evaporation in air at room temperature for 2 days. Main FT-IR absorptions (KBr pellets, cm^{-1}): 3039 (m), 2956 (m), 2927 (w), 2875 (w), 1604 (w), 1566 (w), 1471 (s), 1392 (m), 1352 (m), 1153 (m), 1083 (m), 1035 (w), 941 (w), 804 (s), 736 (s), 707 (m), 621 (w). Mp: > 300 °C. ^{1}H NMR (500 MHz, $CDCl_3$) δ: 9.14 (m, 2H, phen), 9.00 (d, J = 8.1 Hz, phen), 8.50 (d, J = 8.3 Hz, phen), 7.68 (m, 2H, phen), 7.25 (d, 1H, J = 3.8 Hz, thiophene), 7.18 (d, 1H, J = 3.8 Hz, thiophene), 4.64 (m, 2H, *n*-butyl), 2.00 (m,

2H, *n*-butyl), 1.49 (m, 2H, *n*-butyl), 1.00 (m, 3H, *n*-butyl). ^{13}C NMR (125 MHz, $CDCl_3$) δ: 149.0, 147.4, 145.8, 144.9, 144.3, 136.6, 133.3, 130.7, 130.3, 128.2, 127.7, 125.2, 123.7, 125.2, 123.7, 123.5, 122.5, 119.6, 115.7, 46.7, 32.0, 19.7, 13.6. EI-TOF-MS (*m/z*): Calcd for $[C_{21}H_{17}BrN_4S]^+$ 438.0 (100.0 %), 436.0 (98.2 %), found: 438.1 (88.0 %), 436.1 (100.0 %). *Anal.* calcd for $C_{21}H_{17}BrN_4S$: C, 57.67; H, 3.92; N, 12.81 %. Found: C, 57.49; H, 3.96; N, 12.55 %.

General procedure for the syntheses of compounds 6-13 from 5 via Suzuki-Miyaura cross coupling reactions.

A mixture of **5** (0.40 g, 0.92 mmol), boronic acid (1.00 mmol), $Pd(PPh_3)_4$ (0.12 g, 0.10 mmol) and Cs_2CO_3 (1.10 g, 2.76 mmol) was dissolved in a degassed mixture of dioxane (50 mL) and H_2O (5 mL), put into a degassed three-necked flask and refluxed under argon atmosphere for 10 h. After cooled to room temperature, the solution was added into 100 mL $CHCl_3$, and the organic layer was washed with water, dried over anhydrous Na_2SO_4, and concentrated in a vacuum. The desired compounds **6**~1**3** were finally separated by silica gel column chromatography using $CHCl_3$ as the eluent to give corresponding target products in a range of light yellow solid in 25~91 % yields.

Compound **6**: Pale yellow powder in a yield of 0.31 g (78 %). Yellow single crystals of **6** suitable for X-ray diffraction determination were grown from a solution of $CHCl_3/CH_3OH$ by slow evaporation in air at room temperature for 6 days. Mp: > 300 °C. Main FT-IR absorptions (KBr pellets, cm^{-1}): 3037 (m), 2956 (m), 2931 (w), 2873 (w), 1598 (w), 1560 (w), 1471 (s), 1390 (m), 1357 (m), 1213 (w), 1153 (m), 1080 (m), 1035 (w), 941 (w), 804 (s), 736 (s), 707 (m), 615 (w). ^{1}H NMR (500 MHz, $CDCl_3$) δ: 9.16 (s, 2H, phen), 9.05 (d, 1H, J = 8.0 Hz, phen), 8.67 (d, 2H, J = 4.5 Hz, pyridine), 8.53 (d, 1H, J = 8.3 Hz, phen), 7.70 (m, 2H, phen), 7.59 (s, 1H, thiophene), 7.55 (d, 2H, J = 4.5 Hz, pyridine), 7.52 (s, 1H, thiophene), 4.74 (m, 2H, *n*-butyl), 2.10 (m, 2H, *n*-butyl), 1.51 (m, 2H, *n*-butyl), 1.01 (m, 3H, *n*-butyl). ^{13}C NMR (125 MHz, $CDCl_3$) δ: 150.6, 149.2, 147.9, 146.4, 145.0, 144.3, 143.7, 140.5, 136.9, 133.3, 130.4, 128.9, 127.8, 125.8, 125.5, 123.8, 123.5, 119.8, 119.7, 46.9, 32.2, 19.8, 13.6. EI-TOF-MS (*m/z*): Calcd for $[C_{26}H_{21}N_5S]^+$ 435.2 (100.0 %), found 435.3 (100.0 %). *Anal.* calcd for $C_{26}H_{21}N_5S$: C, 71.70; H, 4.86; N, 16.08 %. Found C, 71.56; H, 4.91; N, 15.88 %.

Compound **7**: Pale yellow powder in a yield of 0.37 g (79 %). Yellow single crystals of **7** suitable for X-ray diffraction determination were grown from a mixture solution of $CHCl_3$/EtOH by slow evaporation in air at room temperature for 5 days. Mp:

241-243 °C. Main FT-IR absorptions (KBr pellets, cm^{-1}): 2927 (m), 1722 (s), 1641 (m), 1604 (m), 1560 (w), 1515 (w), 1456 (w), 1398 (m), 1267 (s), 1174 (w), 1107 (m), 1049 (w), 806 (m), 765(m), 738(m), 707 (w). ^{1}H NMR (500 MHz, $CDCl_3$) δ: 9.16 (m, 2H, phen), 9.06 (d, 1H, J = 8.1 Hz, phen), 8.54 (d, 1H, J = 8.3 Hz, phen), 8.11 (d, 2H, J = 8.1 Hz, phenyl), 7.75 (d, 2H, J = 8.1 Hz, phenyl), 7.70 (m, 2H, phen), 7.50 (s, 2H, thiophene), 4.75 (t, 2H, *n*-butyl), 4.42 (m, 2H, ethyl), 2.06 (m, 2H, *n*-butyl), 1.53 (m, 2H, *n*-butyl), 1.42 (t, 3H, ethyl), 1.02 (t, 3H, *n*-butyl). ^{13}C NMR (125 MHz, $CDCl_3$) δ: 166.1, 149.1, 147.8, 145.8, 144.9, 144.3, 137.5, 136.9, 132.2, 130.4, 130.4, 129.9, 129.0, 127.8, 125.6, 125.4, 124.9, 123.8, 123.5, 122.6, 119.7, 61.1, 46.9, 32.2, 19.8, 14.3, 13.6. EI-TOF-MS (*m/z*): Calcd for $[C_{30}H_{26}N_4O_2S]^+$ 506.2 (100.0 %), found 506.3 (100.0 %). *Anal.* calcd for $C_{30}H_{26}N_4O_2S$: C, 71.12; H, 5.17; N, 11.08 %. Found: C, 70.93; H, 5.20; N, 10.97 %.

Compound **8**: Yellowish-green powder in a yield of 0.50 g (90 %).

Compound **9**: Yellowish-green powder in a yield of 0.50 g (91 %). Yellow single crystals of compound **9** suitable for X-ray diffraction determination were grown from a solution of $CHCl_3$ by slow evaporation in air at room temperature for 1 day. Mp: 238-240 °C. Main FT-IR absorptions (KBr pellets, cm^{-1}): 3060 (w), 2927 (m), 2873 (w), 1595 (m), 1500 (m), 1456 (s), 1361 (m), 1234 (m), 1083 (w), 798 (m), 744 (s), 702 (m), 657 (w). ^{1}H NMR (500 MHz, $CDCl_3$) δ: 9.21 (m, 2H), 9.13 (d, 1H, J = 8.1 Hz), 8.60 (d, 1H, J = 8.1 Hz), 8.48 (s, 1H), 8.24 (d, 1H, J = 7.7 Hz), 7.78-7.71 (m, 3H), 7.66 (m, 2H), 7.61 (d, J = 7.8 Hz), 7.55-7.22 (m, 2H), 7.49-7.44 (m, 4H), 7.36 (m, 1H), 4.83 (m, 2H), 2.13 (m, 2H), 1.58 (m, 2H), 1.07 (m, 3H). ^{13}C NMR (125 MHz, $CDCl_3$) δ: 149.0, 148.8, 147.6, 147.5, 144.8, 144.2, 141.5, 140.8, 137.4, 136.9, 130.6, 130.0, 129.6, 129.1, 127.7, 127.0, 126.5, 125.8, 125.3, 124.4, 124.0, 123.4, 123.2, 122.7, 122.6, 120.5, 120.4, 119.9, 117.9, 110.3, 110.1, 46.9, 32.3, 19.8, 13.7. EI-TOF-MS (*m/z*): Calcd for $[C_{39}H_{29}N_5S]^+$ 599.2 (100.0 %), found 599.4 (100.0 %). *Anal.* calcd for $C_{39}H_{31}N_5S$: C, 78.10; H, 4.87; N, 11.68 %. Found: C, 77.92; H, 4.90; N, 11.47 %.

Compound **10**: Pale yellow powder in a yield of 0.30 g (74 %). Yellow single crystals of compound **10** suitable for X-ray diffraction determination were grown from the $CHCl_3$ solution by slow evaporation in air at room temperature for 3 days. Mp: > 300 °C. Main FT-IR absorptions (KBr pellets, cm^{-1}): 3026 (w), 2958 (m), 2952 (w), 2873 (w), 1600 (w), 1560 (m), 1514 (m), 1479 (s), 1456 (m), 1421 (m), 1388 (m), 1155 (w), 1082 (m), 840 (m), 800 (s), 736 (s), 692 (s), 621(w). ^{1}H NMR (500 MHz,

$CDCl_3$) δ: 9.16 (m, 2H, phen), 9.06 (d, 1H, J = 8.0 Hz, phen), 8.55 (d, 1H, J = 8.4 Hz, phen), 7.70 (m, 2H, phen) 7.43 (d, 1H, J = 3.8 Hz, thiophene), 7.31 (d, 2H, J = 4.6 Hz, thiophene), 7.28 (d, 1H, J = 3.8 Hz, thiophene), 7.08 (m, 1H, thiophene), 4.75 (m, 2H, *n*-butyl), 2.06 (m, 2H, *n*-butyl), 1.53 (m, 2H, *n*-butyl), 1.02 (m, 3H, *n*-butyl). ^{13}C NMR (125 MHz, $CDCl_3$) δ: 148.9, 147.6, 146.7, 144.6, 144.0, 140.3, 136.6, 136.3, 130.4, 130.1, 128.4, 127.7, 125.4, 125.3, 124.6, 124.0, 123.7, 123.4, 122.5, 119.6, 46.7, 32.1, 19.7, 13.6. EI-TOF-MS (*m/z*): Calcd for $[C_{25}H_{20}N_4S_2]^+$ 440.1 (100.0 %), found 440.2 (100.0 %). *Anal.* calcd for $C_{25}H_{20}N_4S_2$: C, 68.15; H, 4.58; N, 12.72 %. Found: C, 68.00; H, 5.02; N, 12.55 %.

Compound **11**: Yellow powder in a yield of 0.11 g (26 %). Yellow single crystals of compound **11** suitable for X-ray diffraction determination were grown from a solution of $CHCl_3$ by slow evaporation in air at room temperature for 10 days. Mp: 251-253 °C. Main FT-IR absorptions (KBr pellets, cm^{-1}): 2964 (w), 2931 (w), 2871 (w), 1662 (s), 1512 (w), 1442 (s), 1222 (m), 1049 (w), 802 (m), 742 (m), 663 (w). ^{1}H NMR (500 MHz, $CDCl_3$) δ: 9.93 (s, 1H, formyl), 9.20 (s, 2H, phen), 9.08 (d, 1H, J = 8.1 Hz, phen), 8.59 (d, 1H, J = 8.2 Hz, phen), 7.76 (m, 2H, phen; + 1H, thiophene), 7.50 (s, 1H, thiophene), 7.48 (s, 1H, thiophene), 7.40 (d, 1H, J = 3.7 Hz, thiophene), 4.79 (m, 2H, *n*-butyl), 2.11 (m, 2H, *n*-butyl), 1.57 (m, 2H, *n*-butyl), 1.06 (m, 3H, *n*-butyl). ^{13}C NMR (125 MHz, $CDCl_3$) δ: 182.5, 149.2, 148.0, 146.2, 145.7, 145.0, 144.3, 142.6, 138.7, 137.2, 137.0, 133.3, 133.2, 130.5, 128.6, 127.9, 126.5, 125.7, 125.1, 123.8, 123.6, 122.7, 119.8, 47.0, 32.3, 19.8, 13.6. EI-TOF-MS (*m/z*): Calcd for $[C_{26}H_{20}N_4OS_2]^+$ 468.1 (100.0 %), found 468.2 (100.0 %). *Anal.* calcd for $C_{26}H_{20}N_4OS_2$: C, 66.64; H, 4.30; N, 11.96 %. Found: C, 66.42; H, 4.35; N, 11.78 %.

Compound **12**: Yellow powder in a yield of 0.13 g (31 %). Yellow single crystals of compound **12** suitable for X-ray diffraction determination were grown from a solution of $CHCl_3$ by slow evaporation in air at room temperature for 3 days. Mp: 242-244 °C. Main FT-IR absorptions (KBr pellets, cm^{-1}): 3060 (w), 2960 (w), 2923 (m), 2852 (w), 1666 (s), 1571 (w), 1521 (m), 1471 (m), 1382 (m), 1348 (w), 1274 (w), 1087 (w), 1037 (w), 958 (w), 790 (m), 769 (m), 734 (m), 707 (w). ^{1}H NMR (500 MHz, $CDCl_3$) δ: 9.67 (s, 1H, formyl), 9.16 (m, 2H, phen), 9.03 (d, 1H, J = 8.0 Hz, phen), 8.54 (d, 1H, J = 8.1 Hz, phen), 7.70 (m, 2H, phen) 7.60 (d, 1H, J = 2.7 Hz, thiophene), 7.50 (d, 1H, J = 2.7 Hz, thiophene), 7.33 (d, 1H, J = 2.5 Hz, furan), 6.80 (d, 1H, J = 2.5 Hz, furan), 4.75 (m, 2H, *n*-butyl), 2.06 (m, 2H, *n*-butyl), 1.52 (m, 2H, *n*-butyl), 1.02 (m, 3H, *n*-butyl). ^{13}C NMR (125 MHz, $CDCl_3$) δ: 176.9, 153.6, 151.9, 149.2, 147.9, 146.1,

145.0, 144.3, 136.9, 133.9, 133.6, 130.4, 128.4, 127.8, 126.5, 125.6, 123.8, 123.5, 123.3, 122.6, 119.7, 108.6, 46.9, 32.2, 19.8, 13.6. EI-TOF-MS (*m/z*): Calcd for $[C_{26}H_{20}N_4O_2S]^+$ 452.1 (100.0 %), found 452.1 (100.0 %). *Anal.* calcd for $C_{26}H_{20}N_4O_2S$: C, 69.01; H, 4.45; N, 12.38 %. Found: C, 68.88; H, 4.48; N, 12.21%.

Compound **13**: Pale yellow powder in a yield of 0.41 g (82 %). Yellow single crystals of compound **13** suitable for X-ray diffraction determination were grown from a solution of $CHCl_3$ by slow evaporation in air at room temperature for 3 days. Mp: 266-268 °C. Main FT-IR absorptions (KBr pellets, cm^{-1}): 3062 (w), 2972 (w), 2923 (w), 2871 (w), 1633 (s), 1560 (w), 1444 (m), 1390 (m), 1087 (m), 1045 (m), 798 (m), 746 (s), 707 (w), 621 (w). ^{1}H NMR (500 MHz, $CDCl_3$) δ: 9.20 (m, 2H, phen), 9.11 (d, 1H, J = 8.1 Hz, phen), 8.57 (d, 1H, J = 8.3 Hz, phen), 8.21 (m, 1H, dibenzothiophene), 8.19 (d, 1H, J = 7.8 Hz, dibenzothiophene), 7.92 (m, 1H, dibenzothiophene), 7.77 (m, 2H, thiophene), 7.75 (m, 1H, phen), 7.71 (m, 1H, dibenzothiophene), 7.64 (d, 1H, J = 3.8 Hz, dibenzothiophene), 7.57 (t, 1H, J = 7.7, 15.3 Hz, dibenzothiophene), 7.52 (m, 2H, dibenzothiophene), 4.80 (m, 2H, *n*-butyl), 2.12 (m, 2H, *n*-butyl), 1.58 (m, 2H, *n*-butyl), 1.07 (m, 3H, *n*-butyl). ^{13}C NMR (125 MHz, $CDCl_3$) δ: 149.1, 147.7, 146.9, 145.5, 144.9, 144.3, 139.2, 137.5, 136.9, 136.8, 135.4, 131.5, 130.5, 128.8, 127.8, 127.2, 126.5, 126.2, 125.1, 124.7, 123.9, 123.5, 122.6, 121.8, 121.3, 119.8, 46.9, 32.3, 19.8, 13.7. EI-TOF-MS (*m/z*): Calcd for $[C_{33}H_{24}N_4S_2]^+$ 540.1 (100.0 %), found 540.3 (100.0 %). *Anal.* calcd for $C_{33}H_{24}N_4S_2$: C, 73.30; H, 4.47; N, 10.36 %. Found: C, 73.13; H, 4.51; N, 10.19 %.

Complex **BM3**: $[RuCl_2(p\text{-cymene})]_2$ (0.50 g, 0.82 mmol) and **2** (0.90 g, 1.65 mmol) were added to dry DMF (40 mL), and the mixture was heated at 80 °C under argon atmosphere for 4 h. 4,4'-Dicarboxylic acid-2,2'-bipyridine (dcbpy; 0.40 g, 1.65 mmol) was added and then the reaction mixture was heated at 160 °C for another 4 h in the dark. Excess NH_4NCS was added and the reaction mixture was heated at 130 °C for 5 h. After the reaction, the solvent was removed by a rotary evaporator. Then the solid was dissolved in a basic methanol (tetrabutylammonium hydroxide) solution and purified by the Sephadex LH-20 column with methanol as the eluent to obtain red solid. The red solid was then dissolved in water, and a few drops of 0.02 M HNO_3 were added. The precipitate was filtered and washed thoroughly with distilled water and dried in vacuo, affording the final product **BM3** in a yield of 0.33 g (20 %). Mp > 300 °C. ^{1}H NMR (DMSO-d_6, 500 MHz) δ: 9.61 (s, 1H), 9.52 (s, 1H), 9.18 (s, 1H), 8.99 (s, 1H), 8.38 (s, 1H), 7.84 (m, 4H), 7.61 (m, 4H), 7.51 (m, 3H), 7.34 (m, 4H),

7.08 (m, 6H), 6.98 (d, 2H, J = 7.4 Hz). ESI-MS (*m/z*): 1006.25 (100.0 %) $[M-H]^-$. *Anal.* calcd for $C_{49}H_{31}N_9O_4RuS_3$: C, 58.44; H, 3.10; N, 12.52 %. Found: C, 58.13; H, 3.56; N, 12.28 %.

Complex **BM4**: The synthetic procedure of **BM4** was similar to that described of **BM3**, except that $[RuCl_2(p\text{-cymene})]_2$ (0.21 g, 0.34 mmol), compound **9** (0.40 g, 0.67 mmol), dcbpy (0.16 g, 0.67 mmol) and excess NH_4NCS were used in the reaction. After purification, 0.18 g (25 %) product was obtained. Mp > 300°C. ^{1}H NMR (DMSO-d_6, 500 MHz) δ: 9.67-9.64 (m, 1H), 9.31 (s, 1H), 9.11 (m, 1H), 8.81 (s, 1H), 8.75 (s, 2H), 8.61 (s, 1H), 8.42 (m, 2H), 8.18 (s, 1H), 7.88 (s, 2H), 7.80-7.35 (m, 14H), 5.32 (s, 2H), 5.04 (s, 2H), 2.14 (s, 2H), 1.97 (s, 3H). ESI-MS (*m/z*): 1060.17 (100.0 %) $[M-H]^-$. *Anal.* calcd for $C_{53}H_{37}N_9O_4RuS_3$: C, 59.99; H, 3.51; N, 11.88 %. Found: C, 59.61; H, 4.11; N, 11.46 %.

Electronic Supplementary Information (ESI) available

^{1}H and ^{13}C NMR, EI-TOF-MS and ESI-MS spectra, selected bond lengths (Å) and bond angles (°), and view of the packing structures for related compounds. CCDC nos. 1018234-1018245 contain the supplementary crystallographic data for twelve compounds in this work. These data could be acquired free of charge via www.ccdc.cam.ac.uk/conts/retrieving.html (or from the Cambridge Crystallographic Data Centre, 12 Union Road, Cambridge CB21EZ, UK; fax: [+44]1223-336-033; or deposit @ccdc.cam.ac.uk).

Aacknowledgments

This work was financially supported by the Major State Basic Research Development Programs (Nos. 2013CB922101 and 2011CB933300), the National Natural Science Foundation of China (Nos. 21171088 and 21021062), and the Natural Science Foundation of Jiangsu Province (Grant BK20130054).

Notes and references

1 L. X. Wu and K. Burgess, *J. Am. Chem. Soc.*, 2008, **130**, 4089.

2 M. Y. Lai, C. H. Chen, W. S. Huang, J. T. Lin, T. H. Ke, L. Y. Chen, M. H. Tsai

and C. C. Wu, *Angew. Chem. Int. Ed*., 2008, **47**, 581.

3 S. L. Gong, Y. B. Zhao, M. Wang, C. L. Yang, C. Zhong, J. G. Qin and D. G. Ma, *Chem. Asian J*., 2010, **5**, 2093.

4 O. N. Burchak, L. Mugherli, M. Ostuni, J. J. Lacapere and M. Y. Balakirev, *J. Am. Chem. Soc*., 2011, **133**, 10058.

5 S. J. Jeong, M. K. Kim, S. H. Kim and J. I. Hong, *Org. Electron*., 2013, **14** 2497.

6 L. Yuan, W. Y. Lin, K. B. Zheng and S. S. Zhu, *Accout. Chem. Res*., 2013, **46**, 1462.

7 M. Sarma, T. Chatterjee, S. Ghanta and S. K. Das, *J. Org. Chem*., 2012, **77**, 432.

8 T. Tao, Y. X. Peng, W. Huang and X. Z. You, *J. Org. Chem.*, 2013, **78**, 2472.

9 E. Campioli, C. Rouxel, M. Campanini, L. Nasi, M. Blanchard-Desce and F. Terenziani, *Small*, 2013, **9**, 1982.

10 D. Demeter, V. Jeux, P. Leriche, P. Blanchard, Y. Olivier, J. Cornil, R. Po and J. Roncali, *Adv. Funct. Mater*., 2013, **23**, 4854.

11 A. Leliège, J. Grolleau, M. Allain, P. Blanchard, D. Demeter, T. Rousseau and J. Roncali, *Chem. Eur. J*., 2013, **19**, 9948.

12 S. H. Cheng, S. H. Chou, W. Y. Hung, H. W. You, Y. M. Chen, A. Chaskar, Y. H. Liu and K. T. Wong, *Org. Electron*., 2013, **14**, 1086.

13 S. O. Jeon, K. S. Yook, C. W. Joo and J. Y. Lee, *Adv. Mater.*, 2010, **22**, 1872.

14 A. Keerthi, D. Sriramulu, Y. Liu, C. Thuang, Y. Timothy, Q. Wang and S. Valiyaveettil, *Dyes Pigm*., 2013, **99**, 787.

15 H. J. Tang, Y. H. Li, B. F. Zhao, W. Yang, H. B. Wu and Y. Cao, *Org. Electron*., 2012, **13**, 3211.

16 X. L. Wang, W. Y. Zheng, H. Y. Lin, G. C. Liu, Y. Q. Chen and J. N. Fang, *Tetrahedron Lett*., 2009, **50**, 1536.

17 P. Y. Zhang, L. M. Pei, Y. Chen, W. C. Xu, Q. T. Lin, J. Q. Wang, J. H, Wu, Y. Shen, L. N. Ji and H. Chao, *Chem. Eur. J.*, 2013, **19**, 15494.

18 S. S. Li, C. Zhang, S. Y. Huang, F. Hu, J. Yin and S. H. Liu, *RSC Adv.*, 2012, **2**, 4215.

19 R. M. F. Batista, S. P.G. Costa, S. P.G. Costa, C. Lodeiro and M. M. M. Raposo, *Tetrahedron*, 2008, **64**, 9230.

20 S. Shi, J. Liu, T. M. Yao, X. T. Geng, L. F. Jiang, Q. Y. Yang, L. Cheng and L. N. Ji, *Inorg. Chem.*, 2008, **47**, 2910.

21 P. P. Ren, R. J. Wang, S. Z. Pu, G. Liu and C. B. Fan, *J. Phys. Org. Chem.,* 2014, **27**, 183.

22 R. M. F. Batista, S. P.G. Costa, M. Belsley and M. M. M. Raposo, *Dyes Pigm.*, 2009, **80**, 329.

23 D. Davidson, M. Weiss and M. J. Jelling, *J. Org. Chem.,* 1937, **2**, 319.

24 Z. B. Cai, M. Zhou and J. H. Xu, *J. Mol. Struct*., 2011, **1006**, 282.

25 J. J. Xu, D. Yun and B. Lin, *Synthet. Metal*, 2011, **161**, 1276.

26 J. L. Mathias, H. Arora, R. Lavi, H. Vezin, D. Yufit, M. Orio, N. Aliaga-Alcade and L. Benisvy, *Dalton Trans*., 2013, **42**, 2358.

27 Y. J. Liu and K. Z. Wang, *Eur. J. Inorg. Chem*., 2008, 5214.

28 K. Araki, H. Endo, G. Masuda and T. Ogawa, *Chem. Eur. J*., 2004, **10**, 3331.

29 W. Huang, G. Masuda, S. Maeda, H. Tanaka and T. Ogawa, *Chem. Eur. J.,* 2006, **12**, 607.

30 W. Huang, H. Tanaka and T. Ogawa, *J. Phys. Chem. C*., 2008, **112**, 11513.

31 W. Huang, H. Tanaka, T. Ogawa and X. Z. You, *Adv. Mater.,* 2010, **22**, 2753.

32 Q. Q. Liu, J. Geng, X. X. Wang, K. H. Gu, W. Huang and Y. X. Zheng, *Polyhedron*, 2013, **59**, 52.

33 T. Tao, B. B. Ma, Y. X. Peng, X. X. Wang, W. Huang and X. Z. You, *J. Org. Chem.*, 2013, **78**, 8669.

34 T. Pesnot, L. M. Tedaldi, P. G. Jambrina, E. Rostac and G. K. Wagner, *Org. Biomol. Chem*., 2013, **11**, 6357.

35 . Yuan. Chen, H. C. Lu, C. G. Wu, J. G. Chen, and K. C. Ho, *Adv*. *Funct*. *Mater*. 2007, **17**, 29.

36 . Q. Ji, G. Natu, and Y. Y. Wu, *ACS Appl. Mater. Interfaces*, 2013, **5**, 8641.

37 H. Shahroosvand, F. Nasouti and A. Sousaraei, *Dalton Trans*., 2014, **43**, 5158.

38 Q. Y. Yu, J. F. Huang, Y. Shen, L. M. Xiao, J. M. Liu, D. B. Kuanga and C. Y. Su, *RSC Advances*, 2013, **3**, 19311.

39 S. H. Fan, A. G. Zhang, C. C. Ju, L. H. Gao and K. Z. Wang, *Inorg. Chem*., 2010, **49**, 3752.

40 J. H. Yum, I. Jung, C. Baik, J. J. Ko, M. K. Nazeeruddina and M. Grätzel, *Energy Environ. Sci*., 2009, **2**, 100.

41 C. Y. Chen, J. G. Chen, S. J. Wu, J. Y. Li, C. G. Wu and K. C. Ho. *Angew. Chem. Int. Ed.* 2008, **47**, 7342.

42 B. B. Ma, Y. X. Peng, T. Tao and W. Huang, *Dalton Trans*., 2014, **43**, 16601.

43 A. S. Denisova, M. B. Degtyareva, E. M. Dem'yanchuk and A. A. Simanova, *Russian J. Org. Chem*., 2005, **41**, 1690.

44 K. P. Guo, J. M. Hao, T. Zhang, F. H. Zu, J. F. Zhai, L. Qiu, Z. Zhen, X. H. Liu and Y. Q. Shen, *Dyes Pigm.*, 2008, **77**, 657.

45 Y. L. Li, T. H. Ren and W. J. Dong, *J. Photochem. Photobiol. A Chem.,* 2013, **251**. 1.

46 W. H. Melhuish, *J. Phys. Chem.,* 1961, **65**, 229.

47 SMART and SAINT, Area Detector Control and Integration Software, Siemens

Analytical X-ray Systems Inc., Madison, WI, **2000**.

48 G. M. Sheldrick, SHELXTL (Version 6.10). Software Reference Manual. Madison, Wisconsin (USA): Bruker AXS, Inc., **2000**.

Table of Content

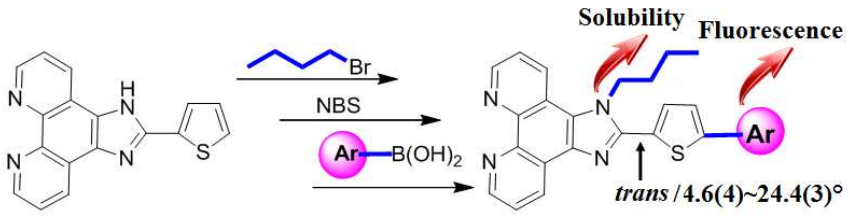

A family of TIP based aromatic heterocyclic compounds has been designed and synthesized by introducing alkyl chains and extended *S*-, *N*- and *O*-containing aromatic heterocyclic tails, where simultaneous enhancement of fluorescence emissions and solubility has been achieved.